

PROCEEDINGS OF SPIE

SPIDigitalLibrary.org/conference-proceedings-of-spie

Nonlinear compression for generation of high energy ultrashort pulses using an Yb-doped large mode area tapered fiber

V. Roy, L. Desbiens, M. Boivin, C. Paré, B. Labranche, et al.

V. Roy, L. Desbiens, M. Boivin, C. Paré, B. Labranche, P. Laperle, Y. Taillon, "Nonlinear compression for generation of high energy ultrashort pulses using an Yb-doped large mode area tapered fiber," Proc. SPIE 10512, Fiber Lasers XV: Technology and Systems, 105120Y (26 February 2018); doi: 10.1117/12.2290104

SPIE.

Event: SPIE LASE, 2018, San Francisco, California, United States

Nonlinear compression for generation of high energy ultrashort pulses using an Yb-doped large mode area tapered fiber

V. Roy*, L. Desbiens, M. Boivin, C. Paré, B. Labranche, P. Laperle, Y. Taillon

INO, 2740 Einstein, Québec, QC, G1P 4S4 Canada

ABSTRACT

Nonlinear compression for generation of high energy ultrashort pulses using an Yb-doped large mode area tapered fiber is reported. Single-stage amplifier gain larger than 43 dB is achieved, with energy of seed pulses (35 ps, 200 kHz) boosted up to 50 μJ at the amplifier output. Spectral broadening induced by self-phase modulation is shown to take place advantageously along the larger end of the counter-pumped active tapered fiber, where the mode area scales beyond 1000 μm^2 . Pulse durations as short as 1 ps and peak powers exceeding 16 MW are demonstrated thereafter using a chirped volume Bragg grating as a dispersive compressor. Efficient suppression of higher-order modes in the large mode area tapered fiber yields diffraction-limited output ($M^2 < 1.2$) for optimal pulse compression.

Keywords: Nonlinear compression, Ultrashort pulse, High energy, Fiber amplifier, Large mode area, Ytterbium, Taper

1. INTRODUCTION

Nowadays ultrashort-pulse laser systems find widespread use in industrial, scientific and medical applications. Fiber-based chirped-pulse amplification systems were shown to yield mJ pulse energy and kW average power in recent years¹⁻². Novel fiber designs with large core sizes and low numerical apertures proved to be effective for mitigating nonlinear effects while simultaneously preserving near diffraction-limited output^{3,4}, both conditions necessary for achieving good contrast ratios after pulse compression. More recently multidimensional coherent combination taking advantage of both spatial and temporal multiplexing was reported to further yield a ten-fold increase in pulse energy⁵. However, systems based on mode-locked oscillators in tandem with chirped pulse amplifiers are often expensive and sometimes difficult to work with, given the complex technology involved and know-how required. Besides, grating-based stretcher/compressor stages are cumbersome given the large footprint occupied, not to mention the odd aspect ratio of the fiber amplifier itself, e.g. in cases where bending is prohibited due to the waveguide geometry.

Nonlinear pulse compression has been shown to benefit as well from advanced fiber designs, for which the potential for scaling pulse energy and peak power stems from the large mode area and reduced optical intensity⁶⁻⁷. As SPM-induced spectral broadening is set to take place before dispersive compression, e.g. following pulse amplification along a rare-earth doped fiber, accumulated nonlinear phase (or B-integral) and resultant frequency up-chirp may proceed to unprecedented peak powers before the onset of adverse effects such as stimulated Raman scattering. Ultimately, self-focusing effect and potentially catastrophic damage will occur, thus preventing from reaching peak powers above a certain threshold. Subsequent pulse compression using a dispersive element such as a chirped volume Bragg grating (VBG) provides decent compression factors with very little space required, which makes the latter convenient for use in industrial lasers⁸⁻⁹. Besides, VBGs were shown to withstand very high powers and are environmentally stable.

It is shown herein how an Yb-doped large mode area (LMA) tapered fiber featuring a depressed-index cladding layer and configured as an ultrafast amplifier can benefit nonlinear pulse compression, with pulse energy and peak power exceeding multi-tens of μJ and MW after compression using a chirped volume Bragg grating. Indeed, not only does adiabatic mode transition along the tapered fiber allows for mitigation of nonlinear effects because of reduced optical intensities, but also counter-pumping of the amplifier is shown to further enhance achievable performances since most of the spectral broadening then takes place at the end of the tapered fiber with expanded mode area exceeding 1000 μm^2 . Details about the active tapered fiber fabricated in-house and its use as an ultrafast amplifier are further provided in the following sections, after which concluding remarks are given.

* vincent.roy@ino.ca; www.ino.ca

2. LMA TAPERED FIBER

Tapered fibers have emerged as a distinct approach in recent years, where scaling to large mode areas naturally occurs along the length of the fiber, often starting as single-mode at launching end¹⁰⁻¹¹. Adiabatic transition of the fundamental mode between the smaller and larger ends of the tapered fiber is expected to yield near diffraction-limited beam profiles at the larger end. The tapering process is usually performed during fiber drawing, leading to great accuracy on core/cladding diameters along the transition between both ends. Large taper ratios were shown recently to give unprecedented mode areas, but most often at the expense of small core/clad ratio and long amplifier fiber length. The latter in turn raises the question of power scalability because of weak pump absorption as well as early onset of nonlinear effects. Besides, irregular index profiles is likely to yield increasingly distorted beam profiles for larger core diameters, sometimes far from being diffraction-limited.

A polarization-maintaining LMA fiber doped with ytterbium and featuring a depressed-index cladding layer was drawn as a long taper, with core/cladding diameter of 35/250 μm in the small end and 56/400 μm in the large end (see Fig. 1(a)-(b)). The core NA was determined to be close to 0.07 from refracted near-field measurement. The effective mode area is predicted to scale from approximately 500 μm^2 in the narrow end to over 1000 μm^2 in the wide end, using a finite-difference mode solver. The taper section supporting adiabatic transition of the mode field between both plateaus is 0.8 m long. Birefringence was measured to be as high as $1.7 \cdot 10^{-4}$. Peak absorption at 976 nm was measured at 10.9 dB/m. A low-index polymer coating was applied over the outer cladding, providing a pump waveguide NA of 0.50. The latter allows for at least 200 W of pump power to be launched from the small end cross-section. Additionally, vignetting of pump light launched from the large end is unlikely to occur with high-brightness pump laser diodes and following underfilled launching conditions, given the small taper ratio.

The refractive index profile of the fiber features a small depression at the inner portion of the 1st cladding layer in order to increase the bending losses of higher order modes (HOMs) relative to those of the fundamental mode¹³. The principle is fairly simple: the higher the index of the outer cladding is, relative to the depressed-index inner cladding layer, the further the evanescent fields of HOMs extend beyond the latter. The index depression relative to the outer cladding has been engineered so as to achieve differential propagation losses between LP₀₁ and LP₁₁ modes exceeding 10 dB/m in the small end of the tapered fiber. With the small end of the tapered fiber coiled to a reasonable diameter (i.e. 14 cm), only the fundamental mode is guided through the adiabatic transition and towards the larger end of the fiber. As a result diffraction-limited beam is expected at the amplifier output. Besides, mode distortion and subsequent reduction of the mode area as a result of fiber bending is estimated below 10 % in the small end. Looser bend radii are required for the larger end though if one is to take advantage of the very large mode area. The taper angle (approx. $2 \cdot 10^{-2}$ mrad) is considered small enough to prevent coupling to HOMs even when the fiber is coiled, as the delineation criteria between adiabatic and lossy tapers calculated from interaction lengths between LP₀₁ mode and HOMs yields taper angles at least a hundred times larger¹⁴.

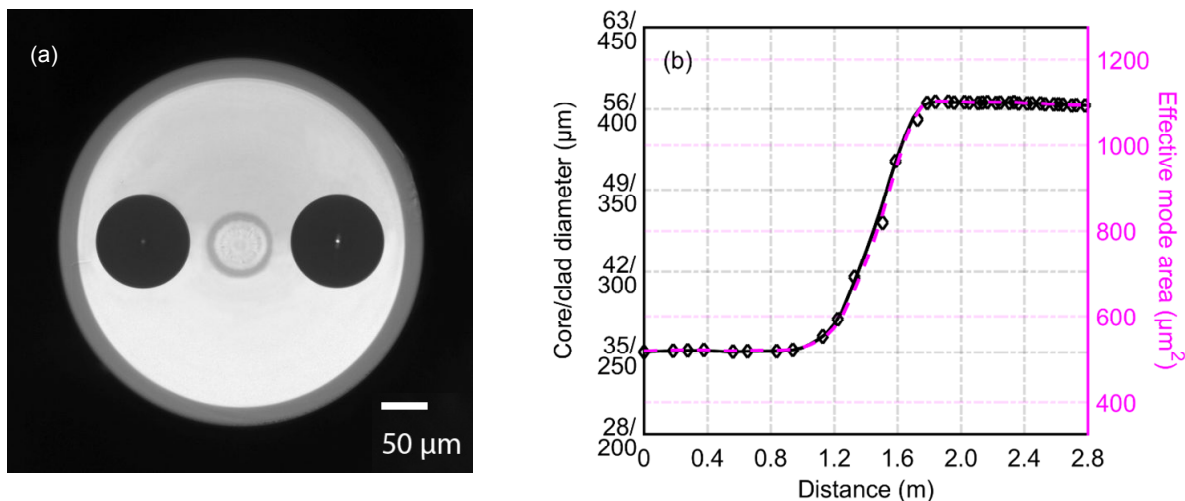


Figure 1 – (a) Optical micrograph of a 56/400 μm section of the LMA tapered fiber and (b) measured core/cladding diameter (straight line) and calculated effective mode area (dashed line) along the tapered fiber (after ref. [12]).

3. NONLINEAR PULSE COMPRESSION

A single-pass high-energy ultrafast amplifier was configured based on the Yb-doped LMA tapered fiber described in the previous section (see Fig. 2). The active fiber was seeded by short optical pulses as generated from a 1064 nm laser diode using external phase modulation and subsequent spectral filtering¹⁵. The oscillator produces nearly chirp-free pulses with duration of about 35 ps (FWHM) as retrieved from the intensity autocorrelation. Pulse repetition frequency could also be adjusted from single-shot up to MHz according to digitized drive current waveforms. The signal was thereafter boosted to nJ level in successive fiber amplifier stages. The gain levels were adjusted so the pulse energy prior to amplification in the tapered fiber would remain fixed regardless of pulse repetition frequency (i.e. 2.5 nJ). Seed pulse energy was kept intentionally small in order to minimize the B-integral accumulated along the tapered fiber. Besides, care was taken to avoid SPM-induced spectral broadening that could potentially take place before amplification in the latter. Dispersion-induced pulse broadening in the pre-amplifier stages was deemed not significant given the pulse duration relative to fiber dispersion.

Alignment of the tapered fiber amplifier was performed with 1064 nm signal light launched from the small end and 976 nm pump light launched from the opposite end, using free-space optics once again to minimize B-integral. Both fiber ends were cut approximately 1 m away from the taper transition, so the total amplifier fiber length was 2.8 m. The fiber output endface was cleaved with an angle of 5° to avoid spurious lasing from excess amplified spontaneous emission whereas the signal input endface was cleaved flat. The small diameter section was coiled on a spool with 14 cm diameter for suppression of HOMs whereas the remainder was loosely coiled (40-50 cm diameter) so as to avoid reduction of the mode area. Wavelength-stabilized pump laser diodes pigtailed with 200 μm – 0.22 NA fiber were used to energize the Yb ions. Preliminary tests with CW signal produced output power exceeding 100 W and slope efficiency of 84 %. The latter is considered as an indication of the absence of vignetting as presumed loss of pump light would otherwise yield lower efficiencies. It is also worth mentioning that a looser coiling at the small end would not bring significant change to the amplifier efficiency.

Pulse energy as high as 50.1 μJ and peak power exceeding 1.3 MW were achieved for 200 kHz seed pulse repetition frequency, thus resulting in single-pass gain greater than 43 dB in the tapered fiber amplifier (see Fig. 3(a)). Amplified spontaneous emission accounted for 15 % of the total output power at most. Output pulse energy was observed to scale down to 40.4 (33.6) μJ while the pulse repetition frequency was increased to 400 (800) kHz. ASE fraction was seen to lessen with increasing pulse repetition frequency. Larger taper ratios would presumably authorize even greater gains and perhaps reduced ASE levels (given that the saturation energy is commensurate with the seed pulse energy for efficient power extraction). Spectral broadening induced by self-phase modulation occurred along with the strong oscillatory modulations characteristic of the phenomenon¹⁶ (see Fig. 3(b)). Accumulated nonlinear phase φ_{NL} (or B-integral) exceeding 20π radians could be inferred from pulse spectra at the amplifier output, with a broadening factor exceeding fifty times the initial bandwidth (> 4 nm). Naturally, φ_{NL} grew larger as ASE lessened with increasing pulse repetition frequency. Red-shifted Stokes line arising from stimulated Raman scattering did show up for output peak powers exceeding 1.5 MW. Understandably the threshold for stimulated Raman scattering was seen to decrease as soon as the seed pulse energy was increased. On the other hand, seed pulses with lower energy would yield soaring ASE fractions, so one in fact has to face a tradeoff between the ASE level and the SRS threshold.

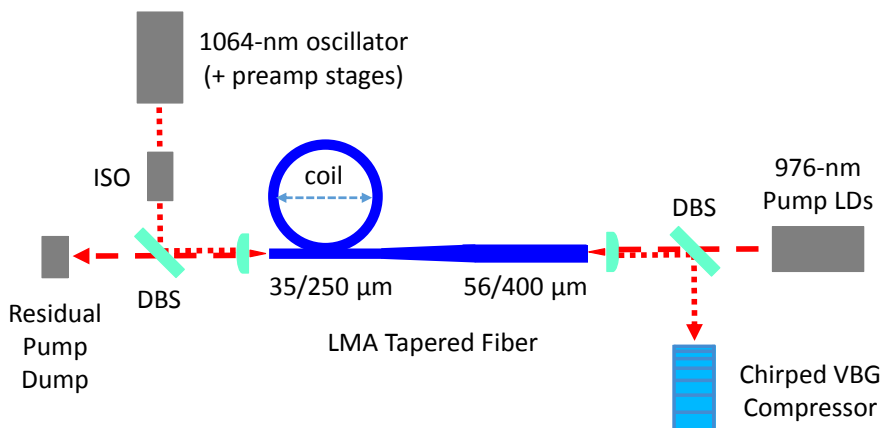


Figure 2 – Schematic representation of the ultrafast amplifier and pulse compressor.

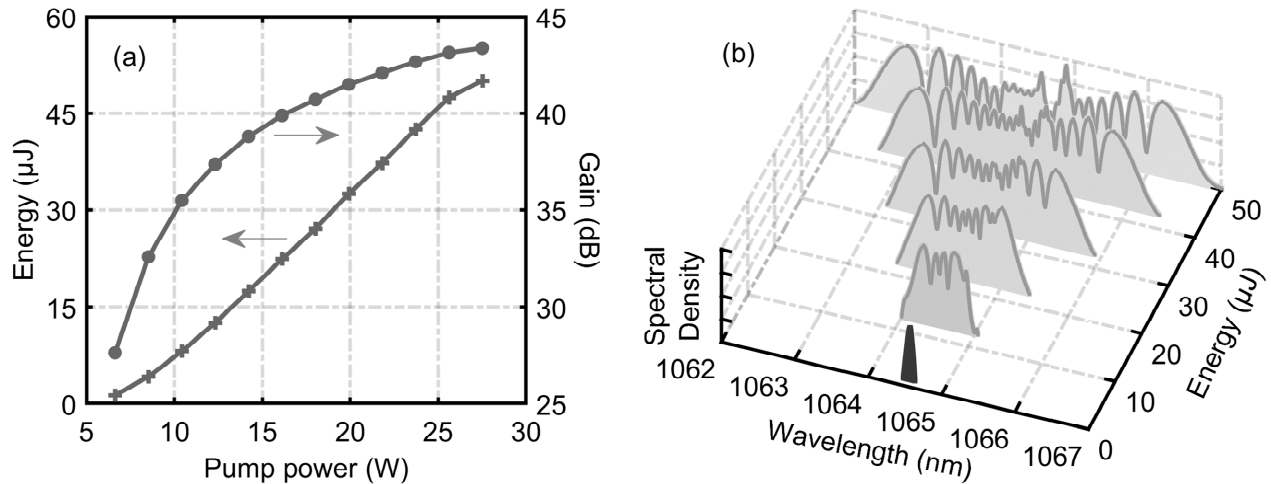


Figure 3 – (a) Pulse energy and amplifier gain achieved with the LMA tapered fiber; (b) SPM-broadened pulse spectra for increasing energy levels at the amplifier output (before compression).

Gain narrowing is believed to bear some importance given the high gain achieved in the tapered amplifier fiber and the ASE reabsorption taking place along the latter. Indeed, the SPM-broadened pulse spectra looked less and less like textbook SPM as the amplifier output power was increased, with the red/blue edges of the spectra somewhat rounded-off (as seen from Fig. 3(b)). Ultimately, gain narrowing is expected to yield slightly longer pulse durations after compression but less prominent pedestal in the vicinity of the autocorrelation peak given that subsequent dispersive compression only matches the linear portion of the frequency chirp prompted by self-phase modulation. In addition, the small distortion in the SPM-broadened spectra results from a superimposed coherent red-shifted CW component which originates from the oscillator (the latter is estimated to carry less than a few percent of the total power).

Pulse compression was performed thereafter using a chirped volume Bragg grating with a dispersive rate designed to match the SPM-induced frequency chirp taking place along the tapered amplifier fiber. The dispersive rate D needed to achieve near optimal compression may be related to pulse duration T_{FWHM} and nonlinear phase φ_{NL} as

$$D = \frac{\pi}{4 \ln 2} \cdot \frac{c}{\lambda^2} \cdot \frac{T_{FWHM}^2}{\varphi_{NL}},$$

where λ is the laser wavelength and c the speed of light. The pulse compressor consists of a polarizing beamsplitter cube, a quarter-wave plate and a chirped VBG. The chirped VBG features a dispersive rate of 5.9 ps/nm, a bandwidth (FWHM) of 7.1 nm and a diffraction efficiency of 88%. Overall transmission of the pulse compressor was estimated to be close to 85%.

Background-free intensity autocorrelation measurements were performed for increasing pulse energies at the compressor output and for different pulse repetition frequencies (see Fig. 4(a)-(b)). The width of the autocorrelation signal τ_{AC} (FWHM) is seen to decrease inversely with the pulse energy (or φ_{NL}), up to the point where SPM-induced chirp matches the dispersion of the pulse compressor. Pulse durations after compression as short as 1 ps (FWHM) were inferred from the background-free intensity autocorrelation measurements, for an impressive compression factor of ≈ 35 . The maximum pulse energy achieved after compression was measured to be just above 42 μ J with pulse repetition frequency of 200 kHz. As the ASE fraction was getting smaller with increasing pulse repetition frequency, the B-integral was seen to grow larger as mentioned above; hence the lower pulse energies obtained following conditions for optimal compression. Besides, in-band ASE light not rejected is estimated to account for only a few percent of the power at the compressor output.

As the chirped VBG may only compensate for the linear part of SPM-induced frequency chirp, which corresponds roughly to the central portion of the optical pulses, some energy is shed away from the central peak after compression. The pedestal below the central peak was seen to carry approximately 47 % of the energy. Compensation of the nonlinear chirp would likely lessen the energy fraction found in the pulse pedestal in proximity of the main peak and therefore lead

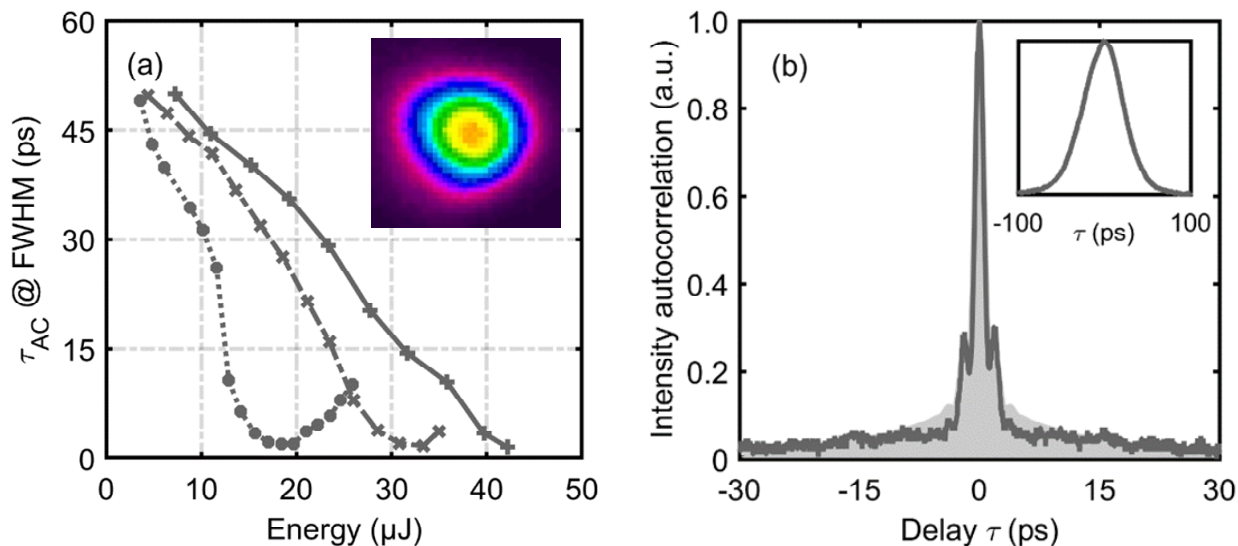


Figure 4 – Intensity autocorrelation after pulse compression (a) for increasing pulse energies and pulse repetition frequencies (straight line: 200 kHz, dash-dotted line: 400 kHz, dotted line: 800 kHz) and (b) for optimal compression, where both experiment (straight line) and simulation (shaded line) results are shown. Insets: beam profile after pulse compressor (left) and intensity autocorrelation before compression (right).

to better contrast ratio after pulse compression. Nevertheless, pulse peak power exceeding 16 MW is estimated when compared with a transform-limited Gaussian pulse of identical duration. Indeed, the fit between theoretically-predicted background-free intensity autocorrelation and actual measurement shown in Fig. 4(b) is quite good. As a reference, the intensity autocorrelation of chirped pulses at the amplifier output is also shown in the same figure as an inset. Efficient suppression of higher-order modes in the LMA tapered fiber is considered beneficial for nonlinear pulse compression, as modal dispersion might otherwise spoil the process with further energy shed away from the central peak into the pedestal. Indeed, near diffraction-limited output was measured after the compressor stage, with $M^2 < 1.2$ as determined using D4 σ method, thus suggesting that the chirped VBG did not significantly affect the beam quality. Besides, the laser beam profile after the pulse compressor stage is shown in the inset of Fig 4(a).

4. CONCLUSION

A single-pass high-energy ultrafast amplifier based on an Yb-doped LMA tapered fiber has been successfully demonstrated. The tapered active fiber fabricated in-house features a mode area exceeding $1000 \mu\text{m}^2$ in its larger end which provide some margin for achieving higher pulse energy and peak power while pushing back the threshold for adverse nonlinear effects such as SRS. Amplifier gain as high as 43 dB were reached, with pulse energy exceeding $50 \mu\text{J}$ and SPM-induced nonlinear phase in excess of 20π rad at the amplifier output. Subsequent dispersive compression using a chirped volume Bragg grating was shown to yield pulse durations as short as 1 ps after compression, corresponding to a compression factor of 35. The energy content in the main peak was verified to exceed 53 % of the total energy, after which peak powers greater than 16 MW could be inferred. According to numbers reported above, this is more than sufficient to drive nonlinear processes such as multiphoton ionization and filamentation in wide-bandgap transparent materials like, e.g., fused silica and sapphire. Besides, power scaling subsequent to rising pulse repetition frequency has been performed easily given the flexible pulse patterns generated by the oscillator. The compact ultrafast amplifier reported herein is considered advantageous in many ways over competing technologies and is therefore believed to find widespread use in many applications.

REFERENCES

- [1] Röser, F., Eidam, T., Rothhardt, J., Schmidt, O., Schimpf, D. N., Limpert, J. and Tünnermann, A., "Millijoule pulse energy high repetition rate femtosecond fiber chirped-pulse amplification system," *Opt. Lett.* 32(24), 3495-3497 (2007).
- [2] Wan, P., Yang, L. M. and Liu, J., "All fiber-based Yb-doped high energy, high power femtosecond fiber lasers," *Opt. Express* 21(24), 29854-29859 (2013).
- [3] Jauregui, C., Limpert, J., Tünnermann, A., "High-power fibre lasers," *Nature Photonics* 7(11), 861-867 (2013).
- [4] Stutzki, F., Jansen, F., Otto, H. J., Jauregui, C., Limpert, J. and Tünnermann, A., "Designing advanced very-large-mode-area fibers for power scaling of fiber-laser systems," *Optica* 1(4), 233-242 (2014).
- [5] Kienel, M., Müller, M., Klenke, A., Limpert, J. and Tünnermann, A., "12 mJ kW-class ultrafast fiber laser system using multidimensional coherent pulse addition," *Opt. Lett.* 41(14), 3343-3346 (2016).
- [6] Martial, I., Papadopoulos, D., Hanna, M., Druon, F. and Georges, P., "Nonlinear compression in a rod-type fiber for high energy ultrashort pulse generation," *Opt. Express* 17(13), 11155-11160 (2009).
- [7] Steinmetz, A., Eidam, T., Nodop, D., Limpert, J. and Tünnermann, A., "Nonlinear compression of Q-Switched laser pulses to the realm of ultrashort durations," *Opt. Express* 19(4), 3758-3764 (2011).
- [8] Glebov, L., Smirnov, V., Rotari, E., Cohanoschi, I., Glebova, L., Smolski, O., Lumeau, J., Lantigua, C. and Glebov, A., "Volume-chirped Bragg gratings: monolithic components for stretching and compression of ultrashort laser pulses," *Opt. Engineering* 53(5), 051514 (2014).
- [9] Yusim, A., Samartsev, I., Shkurikhin, O., Myasnikov, D., Bordenyuk, A., Platonov, N., Kancharla, V. and Gapontsev, V., "New generation of high average power industry grade ultrafast Ytterbium fiber lasers," in *Fiber Lasers XIII: Technology, Systems and Applications*, ed J. Ballato, Proc. of SPIE 9728, 972839 (2016).
- [10] Filippov, V., Chamorovskii, Y., Kerttula, J., Golant, K., Pessa, M. and Okhotnikov, O. G., "Double clad tapered fiber for high power applications," *Opt. Express* 16(3), 1929-1944 (2008).
- [11] Kerttula, J., Filippov, V., Chamorovskii, Y., Ustimchik, V., Golant, K. and Okhotnikov, O. G., "Principles and performance of tapered fiber lasers: from uniform to flared geometry," *Appl. Opt.* 51(29), 7025-7038 (2012).
- [12] Roy, V., Paré, C., Labranche, B., Laperle, P., Desbiens, L., Boivin, M. and Taillon, Y., "Yb-doped large mode area tapered fiber with depressed cladding and dopant confinement," in *Fiber Lasers XIV: Technology, Systems and Applications*, eds C. A. Robin and I. Hartl, Proc. of SPIE 10083, 1008314 (2017).
- [13] Laperle, P., Paré, C., Zheng, H. and Croteau, A., "Yb-doped LMA triple-clad fiber for power amplifiers," in *Fiber Lasers IV: Technology, Systems and Applications*, eds D. J. Harter, A. Tünnermann, J. Broeng and C. Headley III, Proc. SPIE 6453, 645308 (2007).
- [14] Zhu, Y., Eschrich, T., Leich, M., Grimm, S., Kobelke, J., Lorenz, M., Bartelt, H. and Jäger, M., "Yb³⁺-doped rod-type amplifiers with local adiabatic tapers for peak power scaling and beam quality improvement," *Laser Phys.* 27, 105103 (2017).
- [15] Desbiens, L., Drolet, M., Roy, V., Sisto, M. and Taillon, Y., "Arbitrarily-shaped bursts of picosecond pulses from a fiber laser source for high-throughput applications," in *Fiber Lasers VIII: Technology, Systems and Applications*, eds J. W. Dawson and E. C. Honea, Proc. of SPIE 7914, 791420 (2011).
- [16] Agrawal, G. P., *Nonlinear Fiber Optics*, 2nd ed., Academic Press, San Diego, 89-96 (1995).